NV5 GEOSPATIAL
powered by QUANTUM SPATIAL
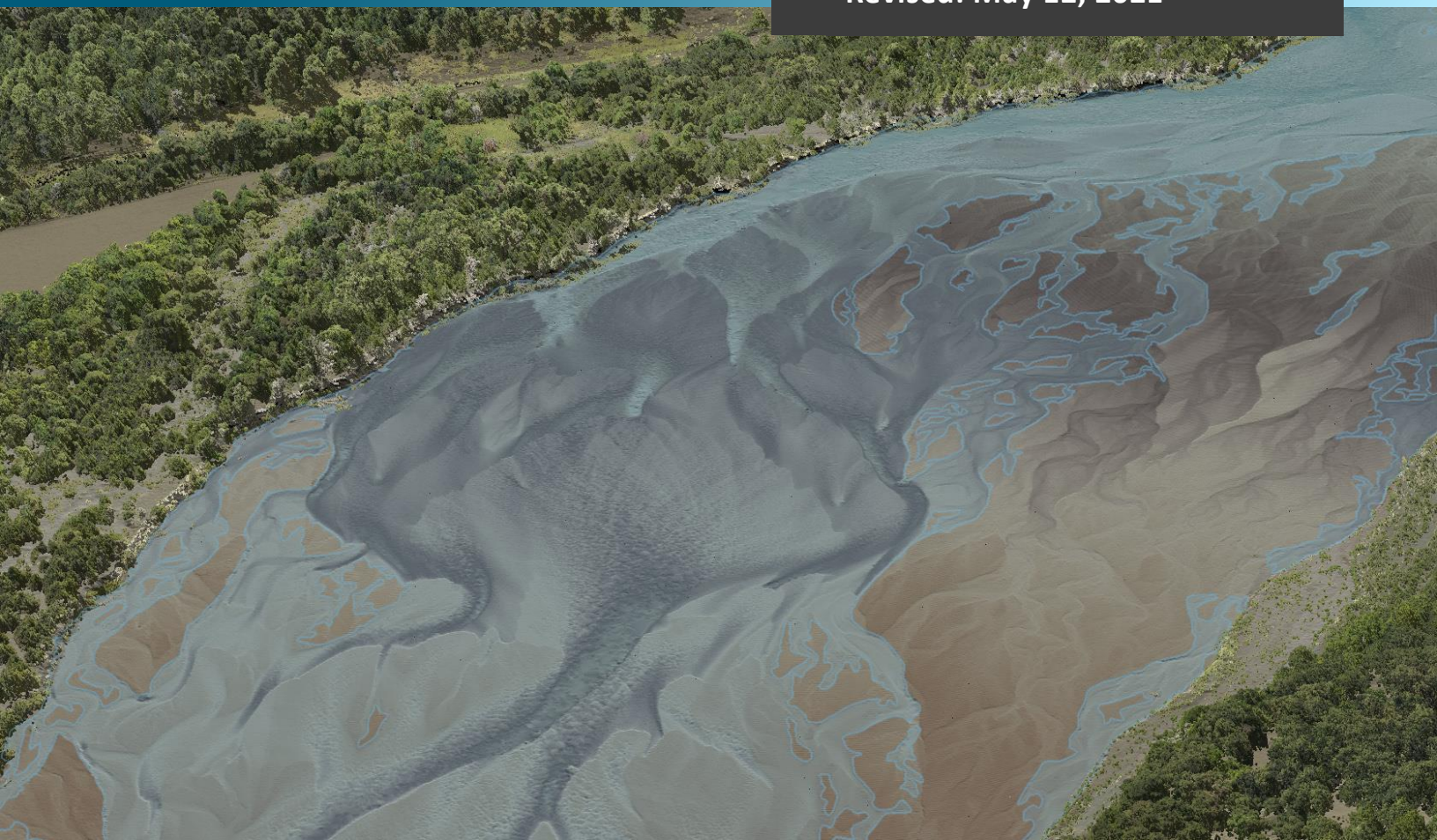
Niobrara River, Nebraska Topobathymetric Lidar

Technical Data Report

Work Package ID: 80391
Work Unit ID: 80388
Contract No. G16PC00016, Order No. 140G0218F0427

Prepared For:

≥USGS
science for a changing world

USGS/NGTOC
Attn: Leslie Lansbery, MS668
1400 Independence Road
Rolla, MO 65401
PH: 573-308-3538

Prepared By:

NV5 GEOSPATIAL
powered by QUANTUM SPATIAL

NV5 Corvallis
1100 NE Circle Blvd, Ste. 126
Corvallis, OR 97330
PH: 541-752-1204

TABLE OF CONTENTS

Cover Photo: A view of the topobathymetric bare earth model colored by elevation, with the lidar point cloud colored by orthoimagery overlaid. Water's edge breaklines are shown in blue.

A view of the Niobrara River in Nebraska, taken by NV5 ground professional Emily Gottesfield.

In September 2018, NV5 Geospatial (NV5) was contracted by the United Stated Geological Survey (USGS) to collect topobathymetric lidar and digital imagery over approximately 92 square miles along the Niobrara River in Nebraska. The Niobrara River area of interest covers an approximately 5-mile long stretch near Valentine, Nebraska, as well as the larger 120-mile corridor which stretches from near Valentine, NE to the river's confluence with the Missouri River. Traditional near-infrared (NIR) lidar and green wavelength (bathymetric) lidar were co-acquired and processed using state-of-the-art sensor technology. In early 2019, widespread flooding along the Missouri and Niobrara Rivers resulted in delaying data acquisition until conditions were deemed suitable by USGS to collect in August of 2020.

This report accompanies the delivered topobathymetric lidar data and imagery, and documents contract specifications, data acquisition procedures, processing methods, and analysis of the final dataset including lidar accuracy and density. Acquisition dates and acreage are shown in Table 1, a complete list of contracted deliverables provided to USGS is shown in Table 2, and the project extent is shown in Figure 1.

Table 1: Acquisition dates, acreage, and data types collected on the Niobrara River

Project Site	Contracted Acres	Buffered Acres	Acquisition Dates	Data Type
Niobrara River, Nebraska	46,686	58,565	August 24 – 28th, 2020 September 1, 2020	Topobathymetric Lidar
			August 24 – 28th, 2020	3 band (RGB) Digital Imagery

Deliverable Products

Table 2: Products delivered to USGS for the Niobrara River project

Niobrara River, Nebraska Lidar Products Projection: UTM Zone 14 North Horizontal Datum: NAD83 (2011) Vertical Datum: NAVD88 (GEOID12B) Units: Meters	
Topobathymetric Lidar	
Points	LAS v 1.4 • All Classified Returns

Rasters	1.0 Meter Cloud Optimized GeoTiffs (*.tif)
	• Topobathymetric Bare Earth Digital Elevation Model (DEM)
	    ○ Clipped
	    ○ Unclipped
	• Highest Hit Digital Surface Models (DSM)
	• Intensity Images
	• Dz Ortho Images

Vectors	Shapefiles (*.shp) • Project Boundary • Lidar Tile Index ESRI File Geodatabase (*.gdb) • Ground Survey Points • Flightline Index • Flightline Swath Coverage Extents • Water's Edge Breaklines • Bathymetric Coverage Shape
3 Band (RGB) Digital Imagery	
Digital Imagery	10 cm Orthophotos • Tiled Imagery Mosaics (*.tif) • AOI Imagery Mosaics (*.sid)
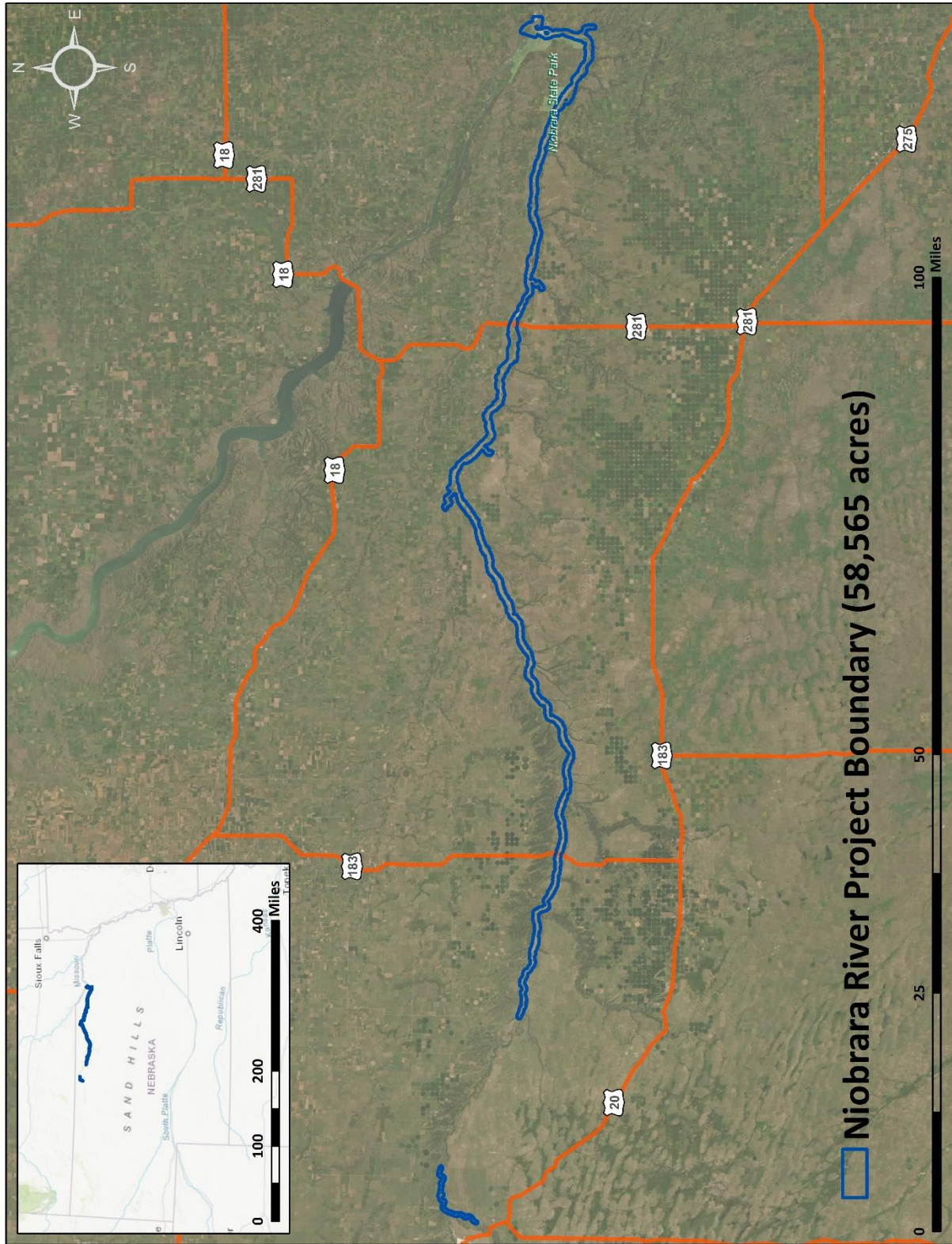
Figure 1: Location map of the Niobrara River site in Nebraska

Niobrara River Project Boundary (58,565 acres)

Technical Data Report – Niobrara River Lidar Project

A scenic photo of the Niobrara River, taken near Valentine, Nebraska.

Planning

In preparation for data collection, NV5 reviewed the project area and developed a specialized flight plan to ensure complete coverage of the Niobrara River Lidar study area at the target combined point density of ≥8 points/m^2. Acquisition parameters including orientation relative to terrain, flight altitude, pulse rate, scan angle, and ground speed were adapted to optimize flight paths and flight times while meeting all contract specifications.

Factors such as satellite constellation availability and weather windows must be considered during the planning stage. Any weather hazards or conditions affecting the flights were continuously monitored due to their potential impact on the daily success of airborne and ground operations. In addition, logistical considerations including private property access, field crew access and safety, and water clarity were reviewed. As part of the planning process, NV5's ground survey team used a Sper Scientific 860040 Turbidity Meter to collect turbidity readings at eleven locations within the project site, as shown in Table 3 and Figure 2 below. Turbidity readings were taken at least three times at each location to verify results.

Sper Scientific 860040 Turbidity Meter

Table 3: Turbidity Scouting Results

| Date	Location	Turbidity 1 (NTU)	Turbidity 2 (NTU)	Turbidity 3 (NTU)	Avg Turbidity
8/22/20	Turb 1	12.12	11.82	12.88	12.27
8/23/20	Turb 1	16.01	15.90	16.75	16.22
8/22/20	Turb 2	11.53	9.73	11.27	10.84
8/23/20	Turb 3	18.21	17.9	17.33	17.81
8/24/20	Turb 3	16.63	17.27	17.37	17.09
8/22/20	Turb 4	13.74	14.02	14.76	14.17
8/25/20	Turb 4	16.34	17.58	17.05	16.99
8/22/20	Turb 5	16.90	17.45	17.37	17.24
8/25/20	Turb 5	22.02	20.79	21.44	21.41
8/25/20	Turb 6	34.89	35.08	37.59	35.85
8/26/20	Turb 7	34.96	34.48	41.0	36.81
8/26/20	Turb 8	54.0	53.0	53.0	53.33
8/27/20	Turb 9	24.99	25.87	28.13	26.33
8/27/20	Turb 10	61.0	60.0	58.0	59.66
8/28/20	Turb 11	11.02	10.57	10.63	10.74
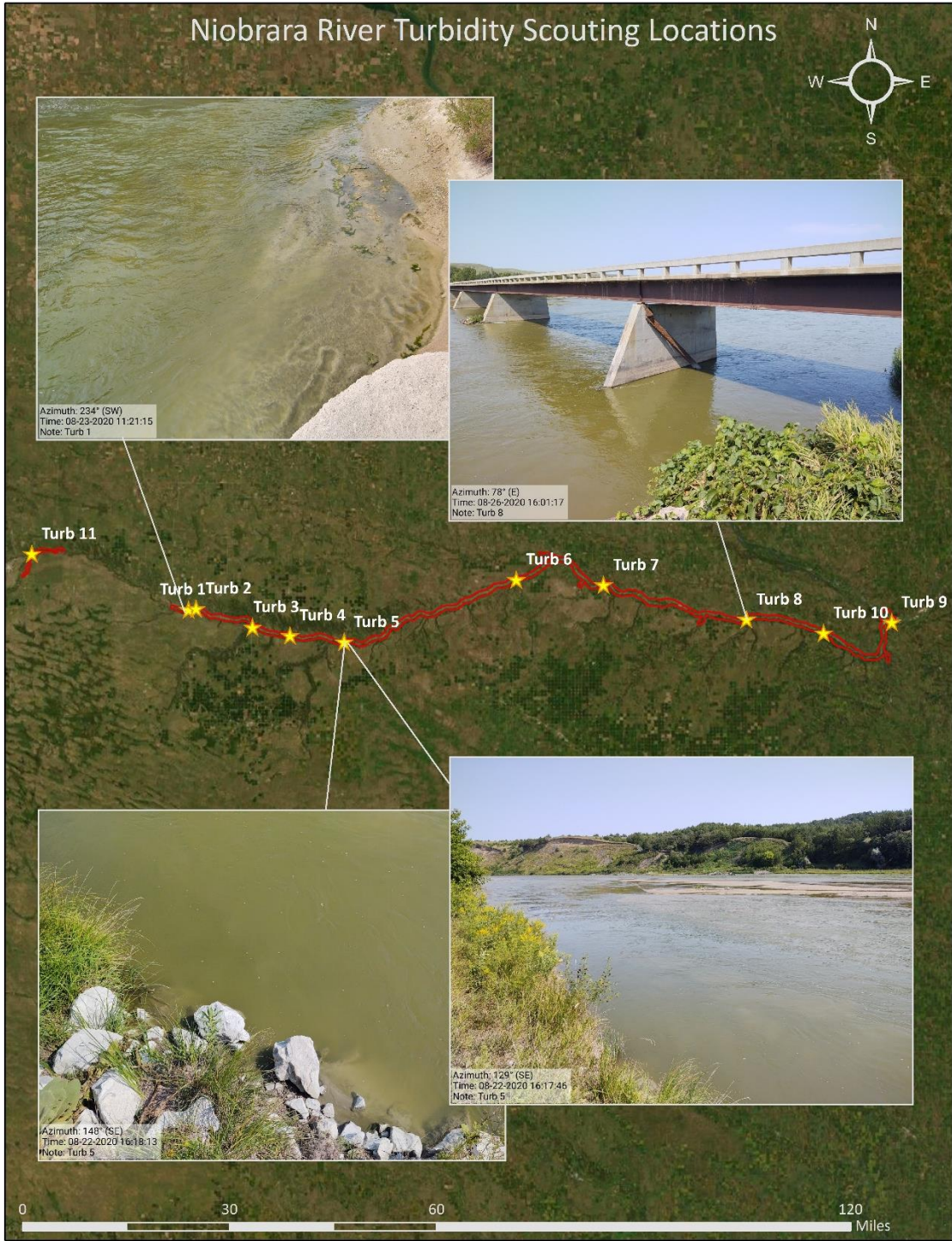
Figure 2: Turbidity Scouting Locations

Airborne Survey

Lidar

The lidar survey was accomplished using a Riegl VQ-880-GII green laser system mounted in a Cessna Caravan. The Riegl VQ-880-GII green wavelength (Λ=532 nm) laser is capable of collecting high resolution topography data, as well as penetrating the water surface with minimal spectral absorption by water. The recorded waveform enables range measurements for all discernible targets for a given pulse. The Riegl VQ-880-GII contains an integrated NIR laser (Λ=1064 nm) that adds additional topography data and aids in water surface modeling. The typical number of returns digitized from a single pulse range from 1 to 15 for the Niobrara River project area. All discernible laser returns were processed for the output dataset. Table 4 summarizes the settings used to yield an average pulse density of ≥8 pulses/m^2 over the Niobrara River project area.

Table 4: Lidar specifications and survey settings

Lidar Survey Settings & Specifications		
Acquisition Dates	8/24/20 – 8/28/20	8/24/20 – 8/28/20
Aircraft Used	Cessna Caravan	Cessna Caravan
Sensor	Riegl	Riegl
Laser	VQ-880GII	VQ-880GII-IR
Maximum Returns	15 returns/pulse	15 returns/pulse
Resolution/Density	Average 8 pulses/m^2	Average 8 pulses/m^2
Nominal Pulse Spacing	0.35 m	0.35 m
Survey Altitude (AGL)	400 m	400 m
Survey speed	145 knots	145 knots
Field of View	40º	42º
Mirror Scan Rate	80 lines per second	Uniform point spacing
Target Pulse Rate	245 kHz	145 kHz
Pulse Length	1.5 ns	3 ns
Laser Pulse Footprint Diameter	28 cm	8 cm
Central Wavelength	532 nm	1064 nm
Pulse Mode	Multiple Times Around (MTA)	Multiple Times Around (MTA)
Beam Divergence	0.7 mrad	0.2 mrad
Swath Width	291 m	307 m
Swath Overlap	30%	30%
Intensity	16-bit	16-bit
Accuracy	RMSE$_Z$ (Non-Vegetated) ≤ 10 cm	
	NVA (95% Confidence Level) ≤ 19.6 cm	
	VVA (95th Percentile) ≤ 30 cm	
	RMSE$_Z$ (Bathymetric) ≤ 30 cm	

All areas were surveyed with an opposing flight line side-lap of ≥30% (≥60% overlap) in order to reduce laser shadowing and increase surface laser painting. To accurately solve for laser point position (geographic coordinates x, y and z), the positional coordinates of the airborne sensor and the attitude of the aircraft were recorded continuously throughout the lidar data collection mission. Position of the aircraft was measured twice per second (2 Hz) by an onboard differential GPS unit, and aircraft attitude was measured 200 times per second (200 Hz) as pitch, roll and yaw (heading) from an onboard inertial measurement unit (IMU). To allow for post-processing correction and calibration, aircraft and sensor position and attitude data are indexed by GPS time (Table 5).

Table 5: Flight Missions by Date

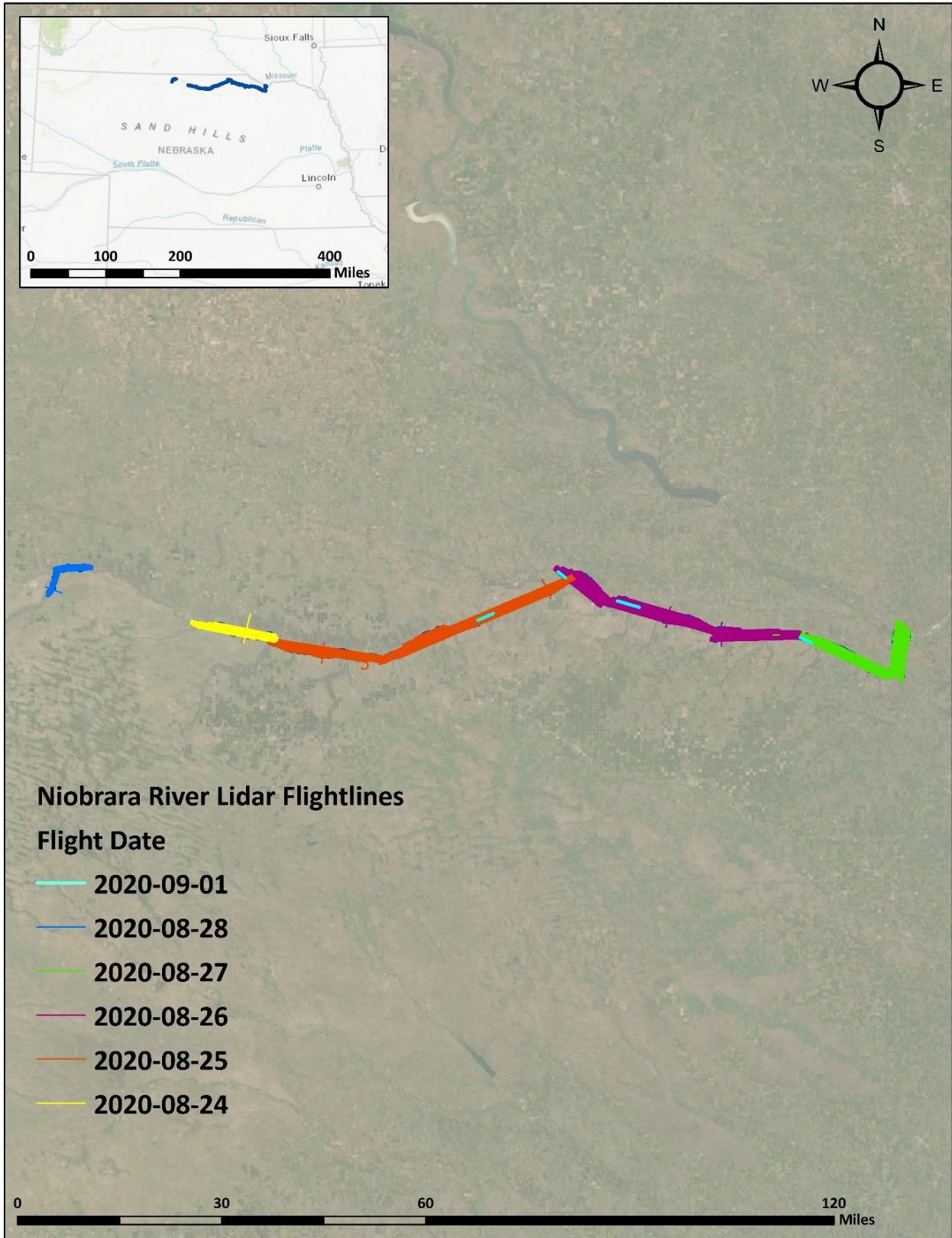| Date	Flight #	Start Time (Adjusted GPS)	End Time (Adjusted GPS)
08/24/2020	1	282295687	282301191
08/25/2020	1	282379303	282396374
08/25/2020	2	282399891	282408738
08/26/2020	1	282468271	282486793
08/26/2020	2	282490350	282491948
08/27/2020	1	282556113	282566506
08/28/2020	1	282642704	282645612
09/01/2020	1	282995233	283007826

Figure 3: Niobrara Flightline Map

Digital Imagery

Aerial imagery was co-acquired with the topobathymetric lidar using a Phase One IXU RS1000 digital camera (Table 6) mounted in a Cessna Caravan. For the Niobrara River site, 14,914 images were collected in three spectral bands (red, green, and blue) with approximately 30% sidelap between frames. The acquisition flight parameters were designed to facilitate a successful lidar survey, but overall pixel resolution was expected to yield ≤ 10 cm. Orthophoto specifications particular to the Niobrara River are shown in Table 7.

Table 6: Camera specifications

Phase One IXU RS1000	
Focal Length	70 mm
Spectral Bands	RGB
CCD Pixel Size	4.6 μm
CCD Array	11,608 x 8,708 pixels
Frame Rate	GPS triggered
Field of View (FOV)	67.4 x 53.2 degrees

Table 7: Niobrara River orthophoto specifications

Digital Orthophotography Specifications	
Equipment	Phase One IXU RS1000
Spectral Bands	Red, Green, Blue
Resolution	10 cm pixel size
Along Track Overlap	variable
Cross Track Overlap	variable
Flight Altitude (MSL)	400 meters
Pixel Depth	8bit

Ground Survey

Ground control surveys, including monumentation and ground survey point (GSP) collection, were conducted to support the airborne acquisition. Ground control data were used to geospatially correct the aircraft positional coordinate data and to perform quality assurance checks on final lidar data.

Base Stations

Base stations were used for collection of ground survey points using real time kinematic (RTK) , post processed kinematic (PPK), and fast static (FS) survey techniques.

Azimuth: 0° (N)
Time: 08-23-2020 10:02:22
Note: USGS_NIOBRARA_01

Figure 4: NV5-established monument USGS_NIOBRARA_01

Base station locations were selected with consideration for satellite visibility, field crew safety, and optimal location for GSP coverage. NV5 utilized two existing permanent active reference stations (CORS), and established six new monuments for the Niobrara River Lidar project (Table 8, Figure 5). New monumentation was set using a 6" Mag nail with an orange "SURVEY MARKER" disk (Figure 4). NV5's professional land surveyor, Steven J. Hyde (NEPLS#769) oversaw and certified the ground survey.

Table 8: Base station positions for the Niobrara River acquisition. Coordinates are on the NAD83 (2011) datum, epoch 2010.00

Base Station ID	Latitude	Longitude	Ellipsoid (meters)	Type
NEAS	42° 31' 35.91685"	-98° 58' 11.18671"	626.146	CORS
NECR	42° 43' 49.72415"	-97° 29' 44.31096"	413.706	CORS
USGS_NIOBRARA_01	42° 46' 58.72204"	-100° 02' 03.20228"	655.369	Monument
USGS_NIOBRARA_02	42° 43' 31.82508"	-99° 44' 54.99657"	623.791	Monument
USGS_NIOBRARA_03	42° 46' 31.86956"	-99° 20' 03.94013"	560.447	Monument
USGS_NIOBRARA_04	42° 50' 36.83486"	-98° 50' 59.44105"	460.904	Monument
USGS_NIOBRARA_05	42° 46' 11.79452"	-98° 26' 32.25951"	404.241	Monument
USGS_NIOBRARA_06	42° 53' 56.47019"	-100° 29' 01.80043"	701.616	Monument

NV5 utilized static Global Navigation Satellite System (GNSS) data collected at 1 Hz recording frequency for each base station. During post-processing, the static GNSS data was triangulated with nearby Continuously Operating Reference Stations (CORS) using the Online Positioning User Service (OPUS[1]) for precise positioning. Multiple independent sessions over the same monument were processed to confirm antenna height measurements and to refine position accuracy.

---

[1] OPUS is a free service provided by the National Geodetic Survey to process corrected monument positions. http://www.ngs.noaa.gov/OPUS/.

Monuments were established according to the national standard for geodetic control networks, as specified in the Federal Geographic Data Committee (FGDC) Geospatial Positioning Accuracy Standards for geodetic networks.[2] This standard provides guidelines for classification of monument quality at the 95% confidence interval as a basis for comparing the quality of one control network to another. The monument rating for this project is shown in Table 9.

Table 9: Federal Geographic Data Committee monument rating for network accuracy

Direction	Rating
1.96 * St Dev $_{NE}$:	0.020 m
1.96 * St Dev $_z$:	0.050 m

For the Niobrara River Lidar project, the monument coordinates contributed no more than 3.4 cm of positional error to the geolocation of the final ground survey points and lidar, with 95% confidence.

Ground Survey Points (GSPs)

Ground survey points were collected using real time kinematic (RTK), post-processed kinematic (PPK), and fast-static (FS) survey techniques. For RTK surveys, a roving receiver receives corrections from a nearby base station or Real-Time Network (RTN) via radio or cellular network, enabling rapid collection of points with relative errors less than 1.5 cm horizontal and 2.0 cm vertical. PPK and FS surveys compute these corrections during post-processing to achieve comparable accuracy. RTK and PPK surveys record data while stationary for at least five seconds, calculating the position using at least three one-second epochs. FS surveys record observations for up to fifteen minutes on each GSP in order to support longer baselines. All GSP measurements were made during periods with a Position Dilution of Precision (PDOP) of ≤ 3.0 with at least six satellites in view of the stationary and roving receivers. A Trimble R10 receiver was utilized to collect ground survey points.

GSPs were collected in areas where good satellite visibility was achieved on paved roads and other hard surfaces such as gravel or packed dirt roads. GSP measurements were not taken on highly reflective surfaces such as center line stripes or lane markings on roads due to the increased noise seen in the laser returns over these surfaces. GSPs were collected within as many flightlines as possible; however, the distribution of GSPs depended on ground access constraints and monument locations and may not be equitably distributed throughout the study area (Figure 5).

Land Cover Class

In addition to ground survey points, non-vegetated and vegetated check points were collected within various land cover classes throughout the study area to evaluate vertical accuracy. Non-vegetated or vegetated check points were collected using a Nikon TotalStation or Trimble R10 Receiver. Vertical accuracy statistics were calculated for all land cover types to assess confidence in the lidar derived ground models across land cover classes (Table 10, see Lidar Accuracy Assessments, page 22).

---

[2] Federal Geographic Data Committee, Geospatial Positioning Accuracy Standards (FGDC-STD-007.2-1998). Part 2: Standards for Geodetic Networks, Table 2.1, page 2-3. http://www.fgdc.gov/standards/projects/FGDC-standards-projects/accuracy/part2/chapter2

Table 10: Land Cover Types and Descriptions

Land Cover Type	Land Cover Code	Example	Description	Accuracy Type
Tall Grass	TALL_GRASS		Herbaceous grasslands in advanced stages of growth	VVA
Shrubland	SHRUB		Areas dominated by herbaceous shrub growth	VVA
Mixed Forest	DEC_FOR MX_FOR		Forested areas dominated by deciduous and/or coniferous species	VVA
Bare Earth	GVL, DRT		Areas of bare earth surface such as gravel or dirt	NVA
Urban	PVD		Areas dominated by urban development, including parks	NVA

Technical Data Report – Niobrara River Lidar Project
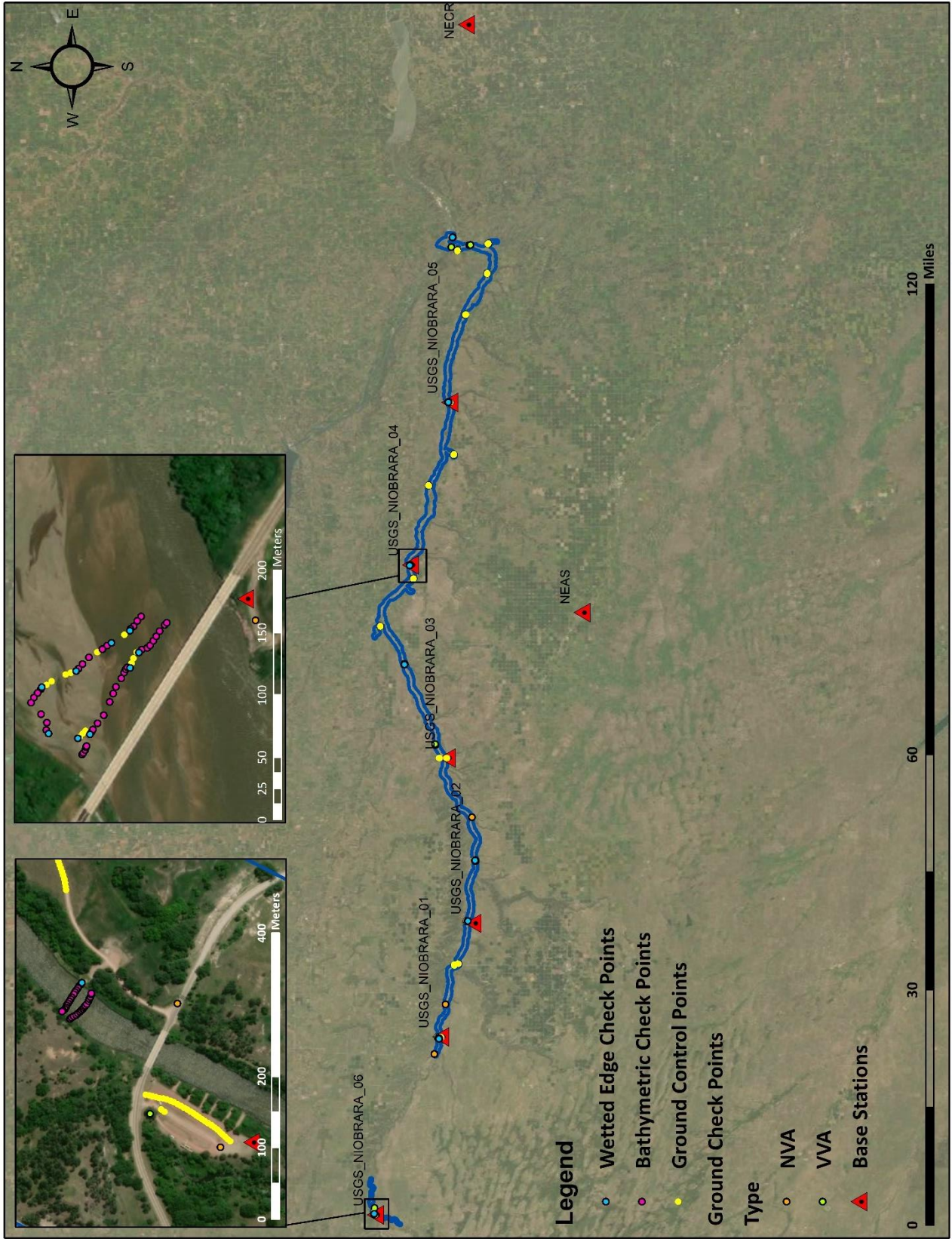
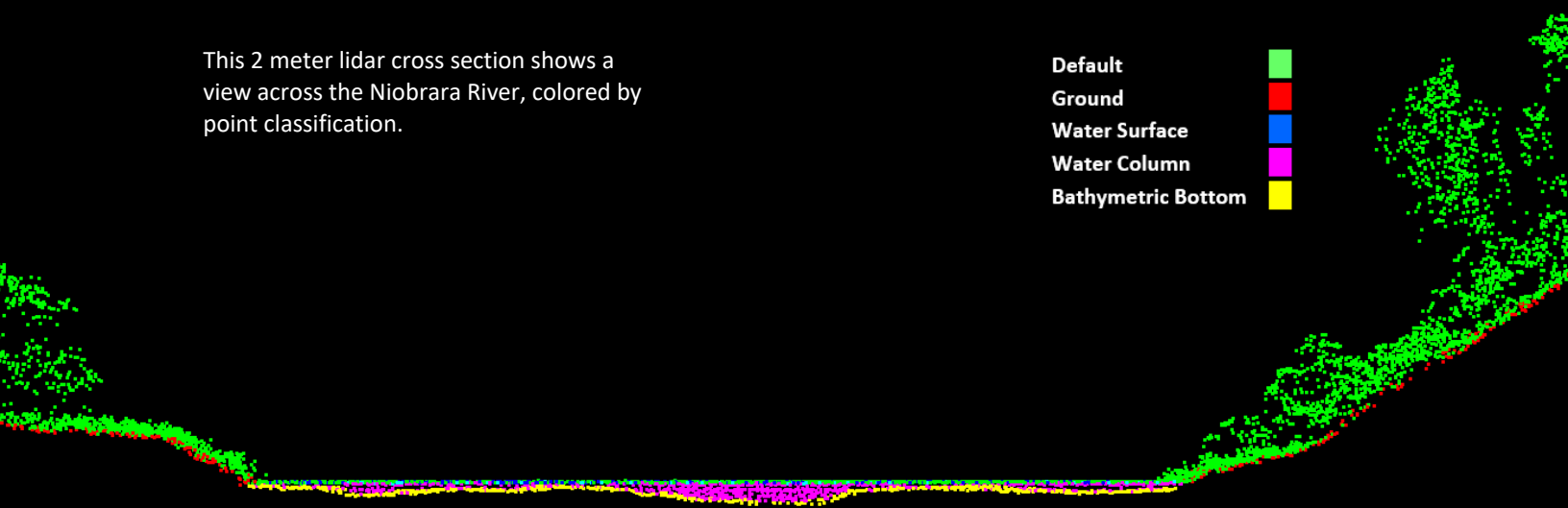**Figure 5: Ground survey location map**

This 2 meter lidar cross section shows a view across the Niobrara River, colored by point classification.

Legend:
- Default (green)
- Ground (red)
- Water Surface (blue)
- Water Column (magenta)
- Bathymetric Bottom (yellow)

Topobathymetric Lidar Data

Upon completion of data acquisition, NV5 processing staff initiated a suite of automated and manual techniques to process the data into the requested deliverables. Processing tasks included GPS control computations, smoothed best estimate trajectory (SBET) calculations, kinematic corrections, calculation of laser point position, sensor and data calibration for optimal relative and absolute accuracy, and lidar point classification (Table 11).

Riegl's RiProcess software was used to facilitate bathymetric return processing. Once bathymetric points were differentiated, they were spatially corrected for refraction through the water column based on the angle of incidence of the laser. NV5 refracted water column points using NV5's proprietary LAS processing software, Las Monkey. The resulting point cloud data was classified using both manual and automated techniques. Processing methodologies were tailored for the landscape. Brief descriptions of these tasks are shown in Table 12.

Table 11: ASPRS LAS classification standards applied to the Niobrara River dataset

Classification Number	Classification Name	Classification Description
1	Default/Unclassified	Laser returns that are not included in the ground class, composed of vegetation and anthropogenic features
1-W	Edge Clip	Laser returns at the outer edges of flightlines that are geometrically unreliable
2	Ground	Laser returns that are determined to be ground using automated and manual cleaning algorithms
7-W	Low Noise	Laser returns that are often associated with artificial points below the ground surface

Classification Number	Classification Name	Classification Description
18-W	High Noise	Laser returns that are often associated with birds and scattering from reflective surfaces
9	Water	Laser returns that are determined to be water using automated and manual cleaning algorithms
40	Bathymetric Bottom	Refracted Riegl sensor returns that fall within the water's edge breakline which characterize the submerged topography
41	Water Surface	Green laser returns that are determined to be water surface points using automated and manual cleaning algorithms
45	Water Column	Refracted Riegl sensor returns that are determined to be water using automated and manual cleaning algorithms

Table 12: Lidar processing workflow

Lidar Processing Step	Software Used
Resolve kinematic corrections for aircraft position data using kinematic aircraft GPS and static ground GPS data. Develop a smoothed best estimate of trajectory (SBET) file that blends post-processed aircraft position with sensor head position and attitude recorded throughout the survey.	POSPac MMS v.8.4
Calculate laser point position by associating SBET position to each laser point return time, scan angle, intensity, etc. Create raw laser point cloud data for the entire survey in *.las (ASPRS v. 1.4) format. Convert data to orthometric elevations by applying a geoid correction.	RiProcess v1.8.5 LidarLauncher1.1 (NV5 proprietary software) Las Monkey 2.6 (NV5 proprietary software)
Import raw laser points into manageable blocks to perform manual relative accuracy calibration and filter erroneous points. Classify ground points for individual flight lines.	TerraScan v.19
Using ground classified points per each flight line, test the relative accuracy. Perform automated line-to-line calibrations for system attitude parameters (pitch, roll, heading), mirror flex (scale) and GPS/IMU drift. Calculate calibrations on ground classified points from paired flight lines and apply results to all points in a flight line. Use every flight line for relative accuracy calibration.	TerraMatch v.19 Las Product Creator 3.0 (NV5 proprietary software)
Apply refraction correction to all subsurface returns.	Las Monkey 2.6 (NV5 proprietary software)
Classify resulting data to ground and other client designated ASPRS classifications (Table 11). Assess statistical absolute accuracy via direct comparisons of ground classified points to ground control survey data.	TerraScan v.19 TerraModeler v.19
Generate bare earth models as triangulated surfaces. Generate highest hit models as a surface expression of all classified points. Export all surface models as cloud optimized geotiffs at a 1 meter pixel resolution.	Las Product Creator 3.0 (NV5 proprietary software) ArcMap v. 10.3.1

Lidar Processing Step	Software Used
Export intensity images as cloud optimized geotiffs at a 1 meter pixel resolution.	ArcMap v. 10.3.1 Las Product Creator 3.0 (NV5 proprietary software)

Bathymetric Refraction

Green lidar pulses that enter the water column must have their position corrected for refraction of the light beam as it passes through the water and its resulting decreased speed. NV5 has developed proprietary software (Las Monkey) to perform this processing based on Snell's law. The first step is to develop a water surface model (WSM) from the NIR lidar water surface returns. The water surface model used for refraction is generated using the NIR channel. Points are filtered and edited to obtain the most accurate representation of the water surface and are used to create a water surface model TIN. A TIN model is preferable to a raster based water surface model to obtain the most accurate angle of incidence during refraction.

Once the WSM is generated, the Las Monkey refraction software then intersects the partially submerged green pulses with the WSM to determine the angle of incidence with the water surface and the submerged component of the pulse vector. This provides the information necessary to correct the position of underwater points by adjusting the submerged vector length and orientation. After refraction, the points are compared against bathymetric check points to assess accuracy.

Water's Edge Breaklines

Water's edge breaklines were created to delineate the land/water interface within the Niobrara River project area. The breaklines were created automatically from post-refracted and post-edited point cloud data. The amount of breakline features was limited by using a >100 square meter threshold for water bodies and a >50 square meter threshold for islands. However, all areas of water went through the refraction process and therefore bathymetric classing exist outside these breaklines

Topobathymetric DEMs

Bathymetric bottom returns can be limited by depth, water clarity, and bottom surface reflectivity. Water clarity and turbidity affects the depth penetration capability of the green wavelength laser with returning laser energy diminishing by scattering throughout the water column. Additionally, the bottom surface must be reflective enough to return remaining laser energy back to the sensor at a detectable level.

As a result, creating digital elevation models (DEMs) presents a challenge with respect to interpolation of areas with no returns. Traditional DEMs are "unclipped", meaning areas lacking ground returns are interpolated from neighboring ground returns (or breaklines in the case of hydro-flattening), with the assumption that the interpolation is close to reality. In bathymetric modeling, these assumptions are prone to error because a lack of bathymetric returns can indicate a change in elevation that the laser can no longer map due to increased depths. The resulting void areas may suggest greater depths, rather than similar elevations from neighboring bathymetric bottom returns. Therefore, NV5 created a water polygon with bathymetric coverage to delineate areas with successfully mapped bathymetry. This shapefile was used to control the extent of the delivered clipped topobathymetric model to avoid false triangulation (interpolation from TIN'ing) across areas in the water with no bathymetric returns.

Digital Imagery

As with the lidar, the collected digital photographs went through multiple processing steps to create final orthophoto products. Initially, a boresight flight was conducted to calculate camera mounting misalignment angles and allow for direct georeferencing of the imagery. Post processed airborne GPS data was linked with image timestamps to resolve exterior orientation (EO) parameters of the camera for all image events used for the Niobrara project. Raw Phase One imagery was geometrically corrected using camera calibration parameters provided by the vendor and output as 8bit, tiff images. Orthophotos were output using the EO and lidar derived bare earth model and finally mosaicked using global color balancing and automatically generated seam lines. Flight planning was optimized for lidar collection which resulted in insufficient image overlap in a few upland areas of the Niobrara AOI. These datagap slivers were all outside of the Niobrara River floodplain. Due to the supplemental nature of the digital imagery deliverables, no manual seam editing or bridge rectification was performed; in some instances where bridges occupy multiple photos or are non nadir to the camera, slight warping is visible. The processing workflow for orthophotos is summarized in Table 13.

Table 13: Orthophoto processing workflow

Orthophoto Processing Step	Software Used
Calculate camera misalignment angles from a system boresight flight conducted close to the Niobrara AOI	Applanix CalQC v8.4
Resolve kinematic corrections for aircraft position data using kinematic aircraft GPS and static ground GPS data. Develop a smoothed best estimate of trajectory (SBET) file that blends post-processed aircraft position with sensor head position and attitude recorded throughout the survey.	Applanix POSPac MMS v8.4
Calculate exterior orientation (EO) for each image event by linking the event time stamps with the SBET and boresight misalignment angles.	Applanix POSPac MMS v8.4
Convert RGB raw (*.iiq) imagery data into geometrically corrected 3 band, TIFF files.	iX Capture v3.4
Import DEM and generate individual ortho images.	Inpho OrthoMaster v10.1
Mosaic orthorectified imagery, blending seams between individual photos and correcting for radiometric differences between them.	OrthoVista/SeamEditor v10.1

Only Echo
First of Many
Intermediate
Last of Many
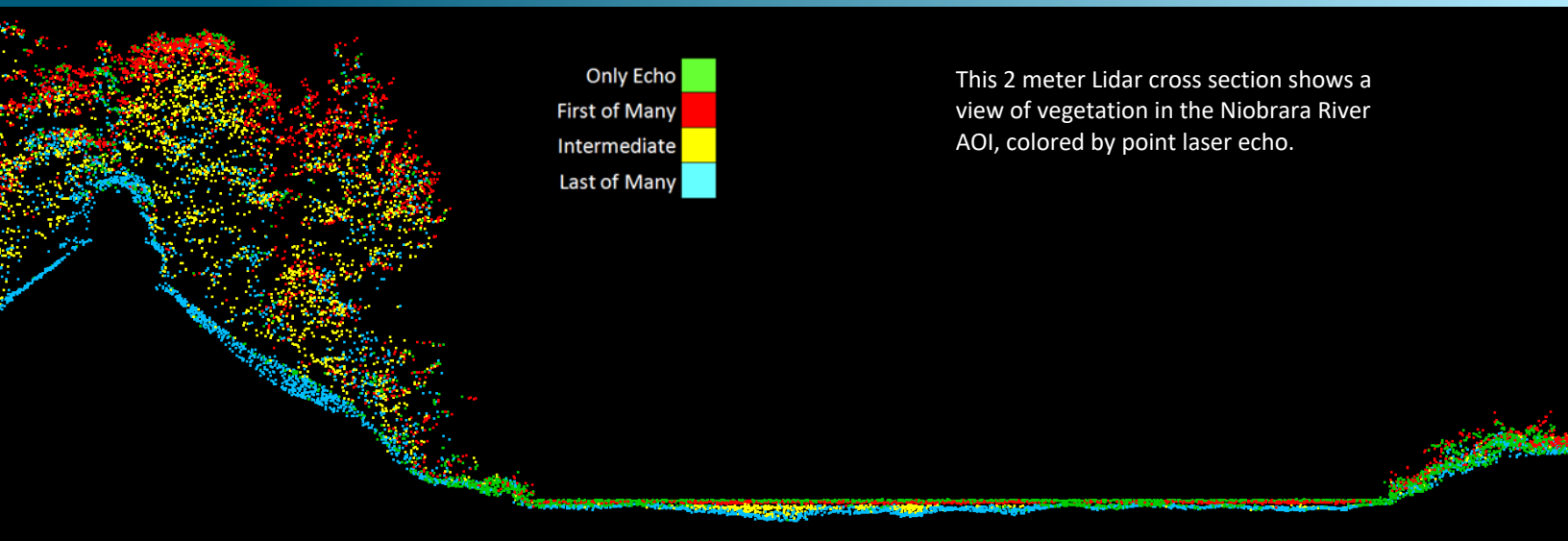
This 2 meter Lidar cross section shows a view of vegetation in the Niobrara River AOI, colored by point laser echo.

Lidar Point Density

First Return Point Density

The acquisition parameters were designed to acquire an average first-return density of 8 points/m^2. First return density describes the density of pulses emitted from the laser that return at least one echo to the system. Multiple returns from a single pulse were not considered in first return density analysis. Some types of surfaces (e.g., breaks in terrain, water and steep slopes) may have returned fewer pulses than originally emitted by the laser.

First returns typically reflect off the highest feature on the landscape within the footprint of the pulse. In forested or urban areas the highest feature could be a tree, building or power line, while in areas of unobstructed ground, the first return will be the only echo and represents the bare earth surface.

The average first-return density of the Niobrara River Lidar project was 19.28 points/m^2 (Table 14). The statistical and spatial distributions of all first return densities per 100 m x 100 m cell are portrayed in Figure 6 and Figure 7.

Bathymetric and Ground Classified Point Densities

The density of ground classified lidar returns and bathymetric bottom returns were also analyzed for this project. Terrain character, land cover, and ground surface reflectivity all influenced the density of ground surface returns. In vegetated areas, fewer pulses may have penetrated the canopy, resulting in lower ground density. Similarly, the density of bathymetric bottom returns was influenced by turbidity, depth, and bottom surface reflectivity. In turbid areas, fewer pulses may have penetrated the water surface, resulting in lower bathymetric density.

The ground and bathymetric bottom classified density of lidar data for the Niobrara River project was 7.10 points/m^2(Table 14). The statistical and spatial distributions ground classified and bathymetric bottom return densities per 100 m x 100 m cell are portrayed in Figure 8 and Figure 9.

Table 14: Average lidar point densities

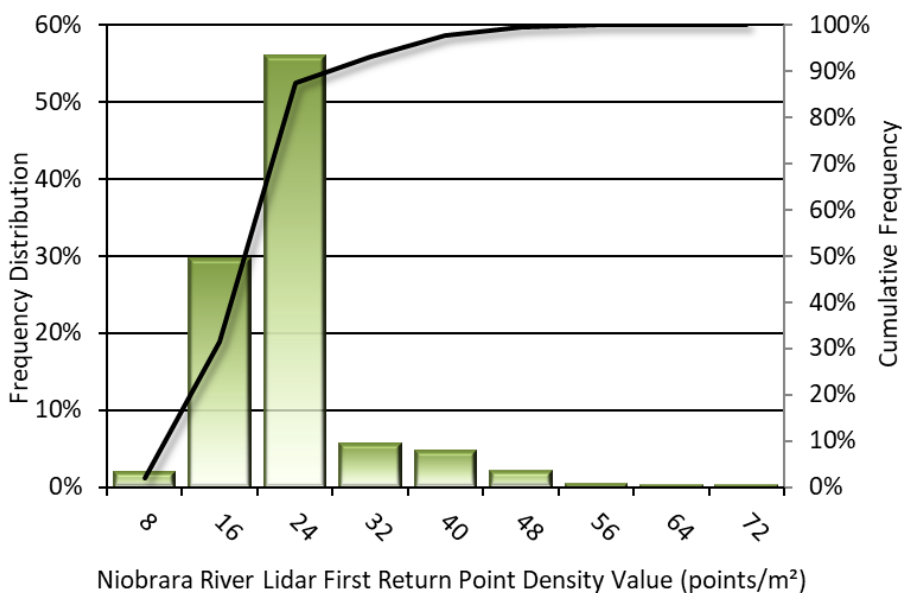| Density Type	Point Density
First Returns	19.28 points/m²
Ground and Bathymetric Bottom Classified Returns	7.10 points/m²

Figure 6: Frequency distribution of first return densities per 100 x 100 m cell
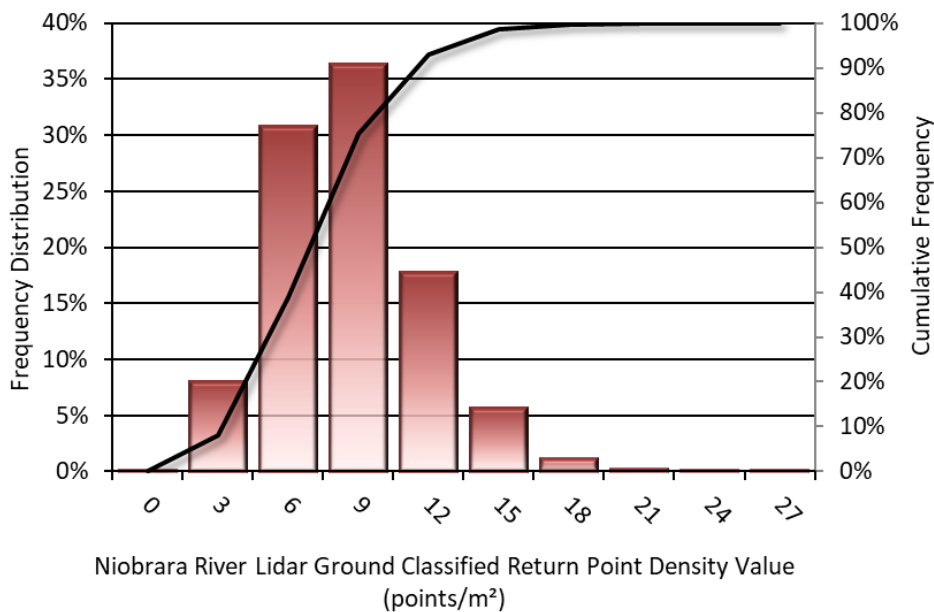

Figure 7: Frequency distribution of ground and bathymetric bottom classified return densities per 100 x 100 m cell
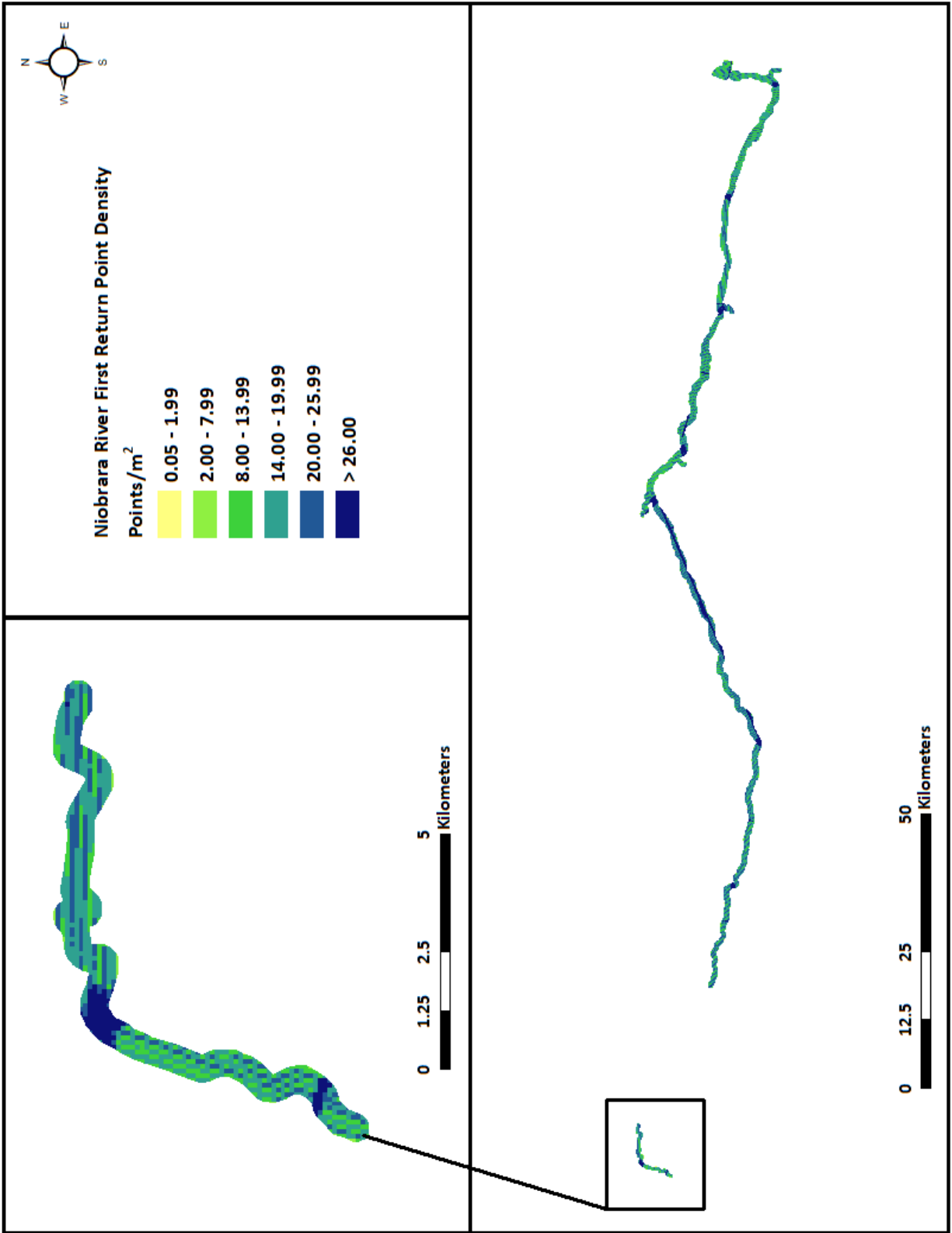
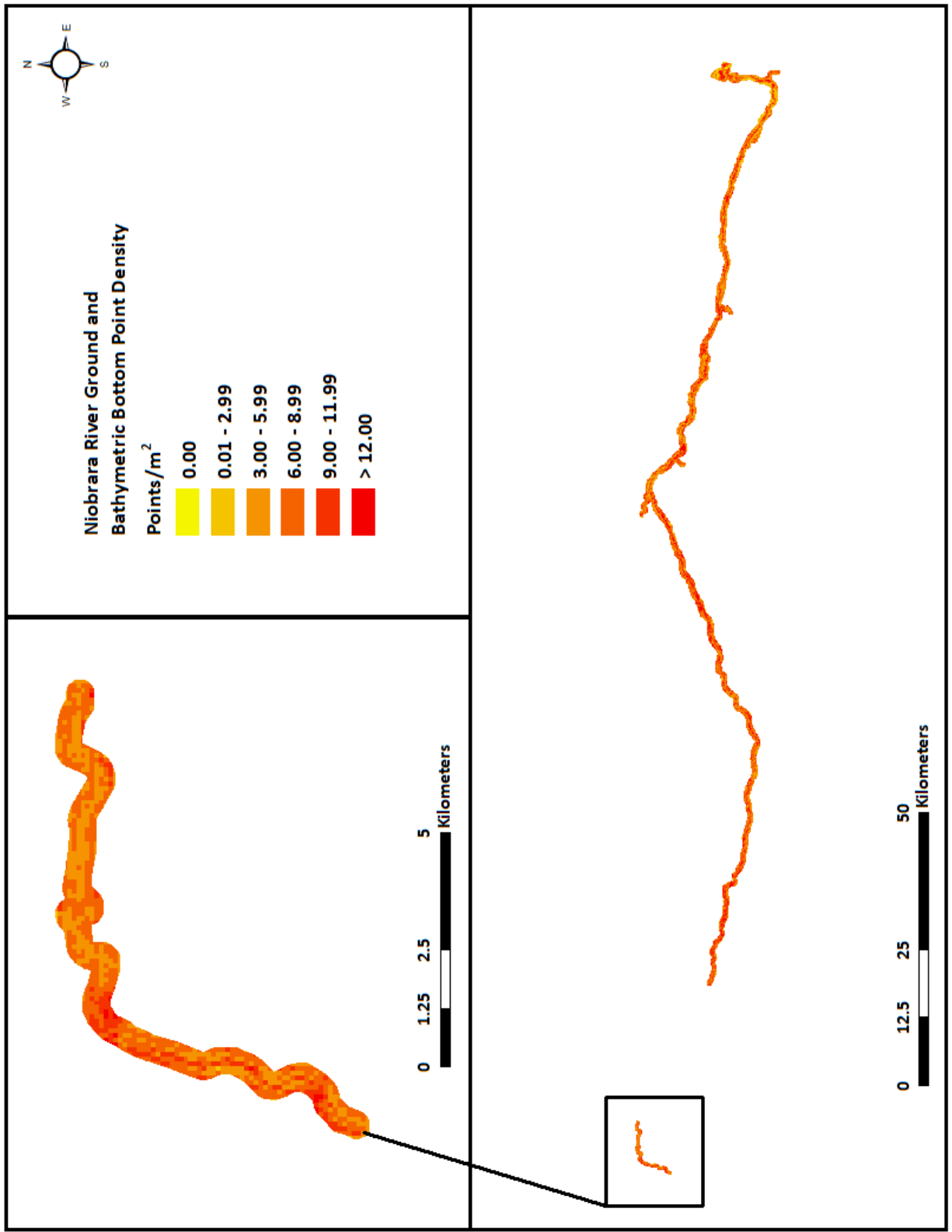**Figure 8: First return density map for the Niobrara River site (100 m x 100 m cells)**

Figure 9: : Ground and bathymetric bottom density map for the Niobrara River site (100 m x 100 m cells)

Lidar Accuracy Assessments

The accuracy of the lidar data collection can be described in terms of absolute accuracy (the consistency of the data with external data sources) and relative accuracy (the consistency of the dataset with itself). See Appendix A for further information on sources of error and operational measures used to improve relative accuracy.

Lidar Non-Vegetated Vertical Accuracy

Absolute accuracy was assessed using Non-vegetated Vertical Accuracy (NVA) reporting designed to meet guidelines presented in the FGDC National Standard for Spatial Data Accuracy[3]. NVA compares known ground check point data that were withheld from the calibration and post-processing of the lidar point cloud to the triangulated surface generated by the unclassified lidar point cloud as well as the derived gridded bare earth DEM. NVA is a measure of the accuracy of lidar point data in open areas where the lidar system has a high probability of measuring the ground surface and is evaluated at the 95% confidence interval (1.96 * RMSE), as shown in Table 15.

The mean and standard deviation (sigma σ) of divergence of the ground surface model from ground check point coordinates are also considered during accuracy assessment. These statistics assume the error for x, y and z is normally distributed, and therefore the skew and kurtosis of distributions are also considered when evaluating error statistics. For the Niobrara River survey, 24 ground check points were withheld from the calibration and post-processing of the lidar point cloud, with resulting non-vegetated vertical accuracy of 0.066 meters, as compared to the classified LAS and 0.065 meters against the bare earth DEM, with 95% confidence (Figure 10 and Figure 11).

NV5 also assessed absolute accuracy using 650 ground control points. Although these points were used in the calibration and post-processing of the lidar point cloud, they still provide a good indication of the overall accuracy of the lidar dataset, and therefore have been provided in Table 15 and Figure 12.

Table 15: Absolute accuracy results

Absolute Vertical Accuracy			
	NVA, as compared to Classified LAS	**NVA, as compared to Bare Earth DEM**	**Ground Control Points**
Sample	24 points	24 points	650 points
95% Confidence (1.96*RMSE)	0.066 m	0.065 m	0.059 m
Average	-0.002 m	-0.008 m	-0.002 m
Median	-0.003 m	-0.007 m	0.004 m
RMSE	0.034 m	0.033 m	0.030 m
Standard Deviation (1σ)	0.035 m	0.033 m	0.030 m

---

[3] Federal Geographic Data Committee, ASPRS POSITIONAL ACCURACY STANDARDS FOR DIGITAL GEOSPATIAL DATA EDITION 1, Version 1.0, NOVEMBER 2014.
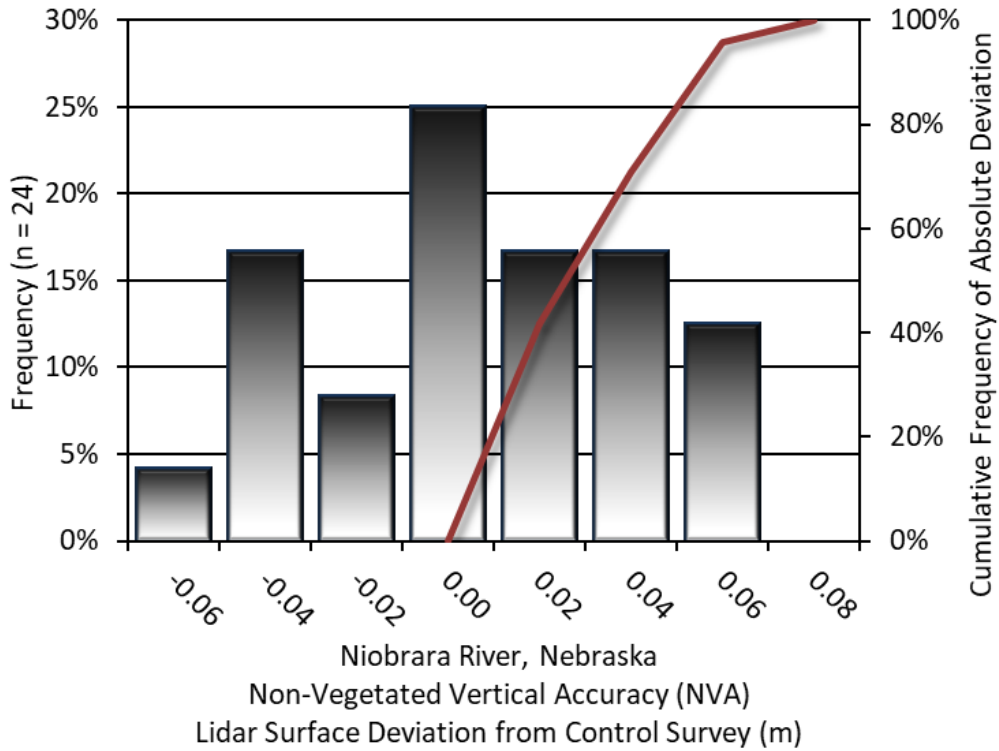https://www.asprs.org/a/society/committees/standards/Positional_Accuracy_Standards.pdf.

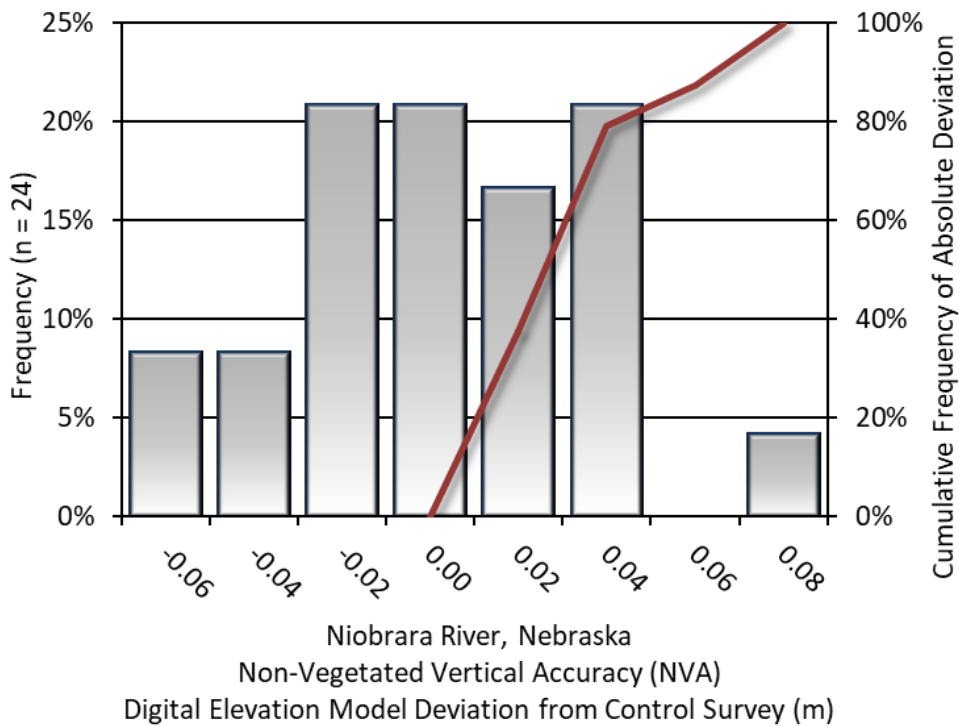**Figure 10: Frequency histogram for unclassified LAS deviation from ground check point values**

Figure 11: Frequency histogram for lidar bare earth DEM deviation from ground check point values
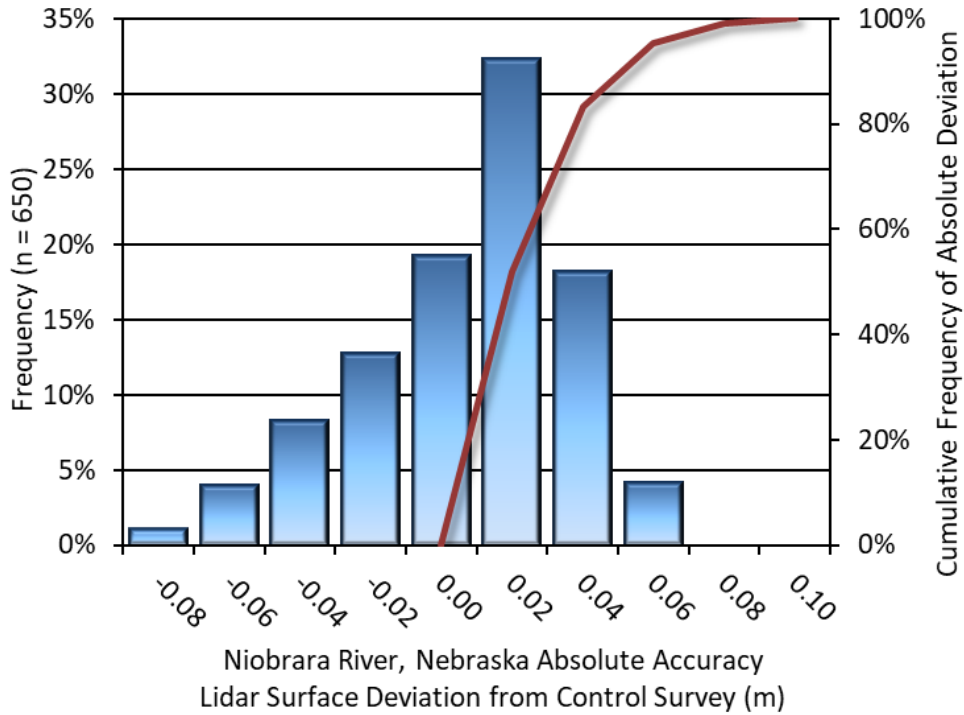
Figure 12: Frequency histogram for lidar surface deviation ground control point values

Lidar Bathymetric Vertical Accuracies

Bathymetric (submerged or along the water's edge) check points were also collected in order to assess the submerged surface vertical accuracy (Table 16, Figure 13, and Figure 14). Assessment of 309 submerged bathymetric check points resulted in a vertical accuracy of 0.143 meters, while assessment of 39 wetted edge check points resulted in a vertical accuracy of 0.065 meters, evaluated at 95% confidence interval.

Table 16: Bathymetric Vertical Accuracy for the Niobrara River Project

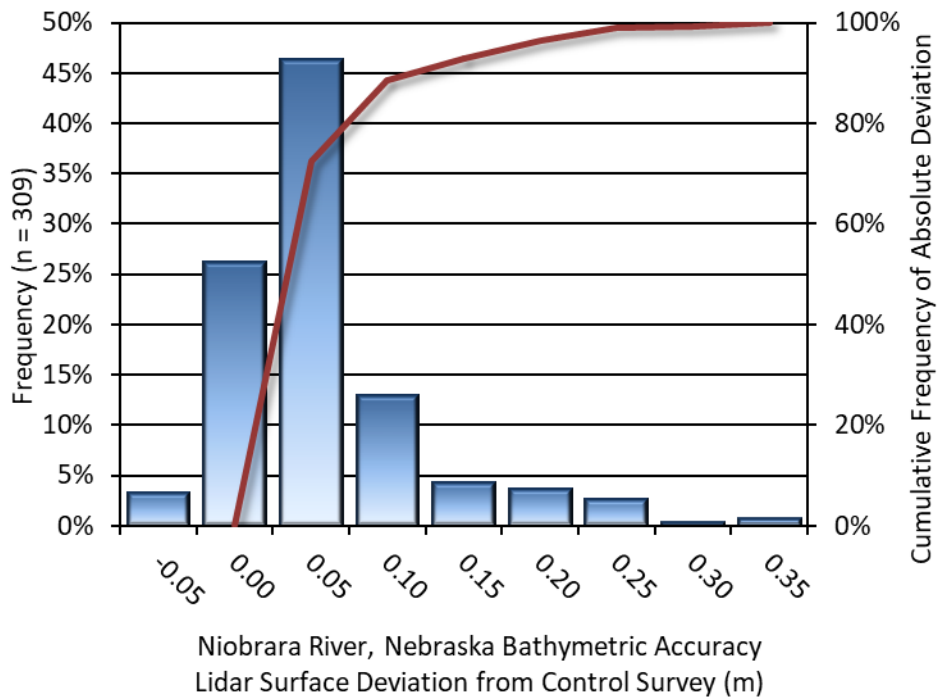| Bathymetric Vertical Accuracy (VVA)		
	Submerged Bathymetric Check Points	**Wetted Edge Bathymetric Check Points**
Sample	309 points	39 points
95% Confidence (1.96*RMSE)	0.143 m	0.065 m
Average Dz	0.033 m	-0.004 m
Median	0.020 m	-0.002 m
RMSE	0.073 m	0.033 m
Standard Deviation (1σ)	0.065 m	0.034 m

Figure 13: Frequency histogram for lidar surface deviation from submerged check point values
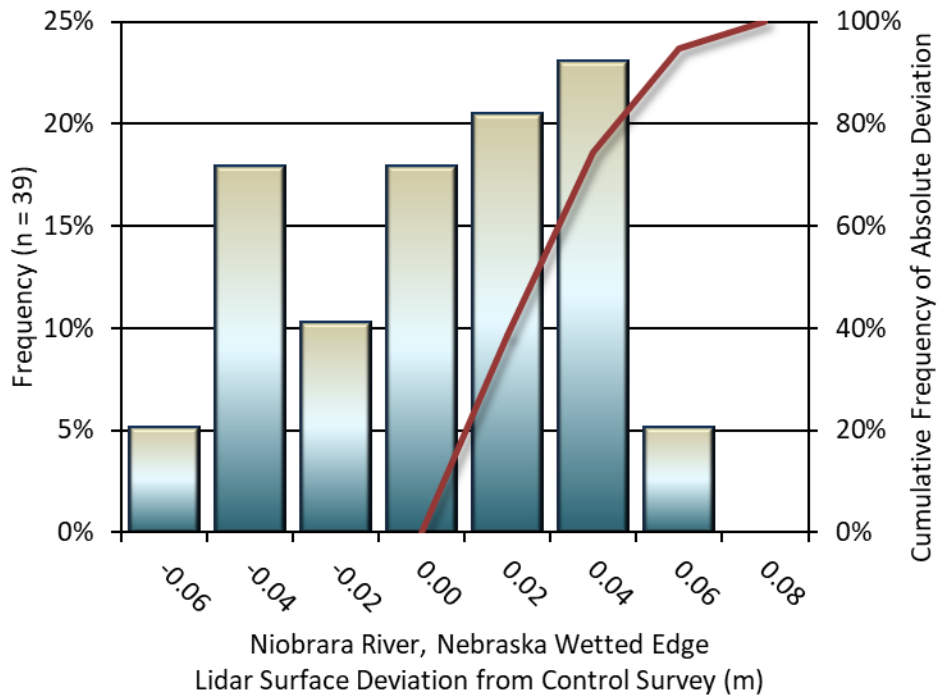

Figure 14: Frequency histogram for lidar surface deviation from wetted edge check point values
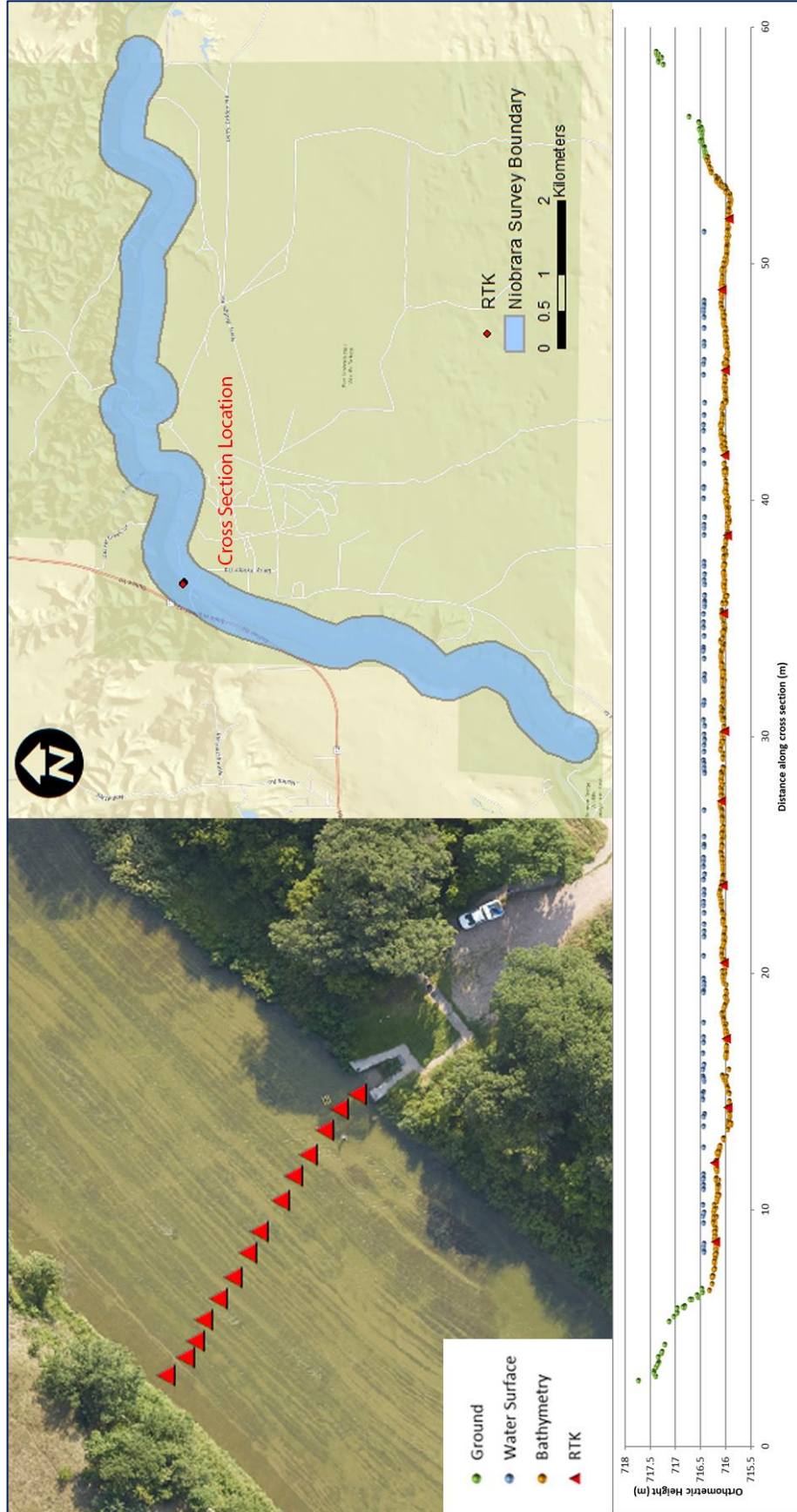
Figure 15: This figure displays the close vertical and horizontal alignment between collected submerged bathymetric check points, and the mapped Lidar returns in the Niobrara River channel.

Lidar Vegetated Vertical Accuracies

NV5 Geospatial also assessed vertical accuracy using Vegetated Vertical Accuracy (VVA) reporting. VVA compares known ground check point data collected over vegetated surfaces using land class descriptions to the triangulated ground surface generated by the ground classified lidar points. For the Niobrara River survey, 11 vegetated check points were collected, with resulting vegetated vertical accuracy of 0.212 meters as compared to the classified LAS, and 0.202 meters as compared to the bare earth DEM evaluated at the 95th percentile (Table 17, Figure 16, Figure 17).

Table 17: Vegetated vertical accuracy results

Vegetated Vertical Accuracy		
	VVA, as compared to classified LAS	**VVA, as compared to bare earth DEM**
Sample	11 points	11 points
95th Percentile	0.212 m	0.202 m
Average	0.099 m	0.088 m
Median	0.088 m	0.071 m
RMSE	0.126 m	0.120 m
Standard Deviation (1σ)	0.082 m	0.086 m

Niobrara River, Nebraska Vegetated Vertical Accuracy (VVA)
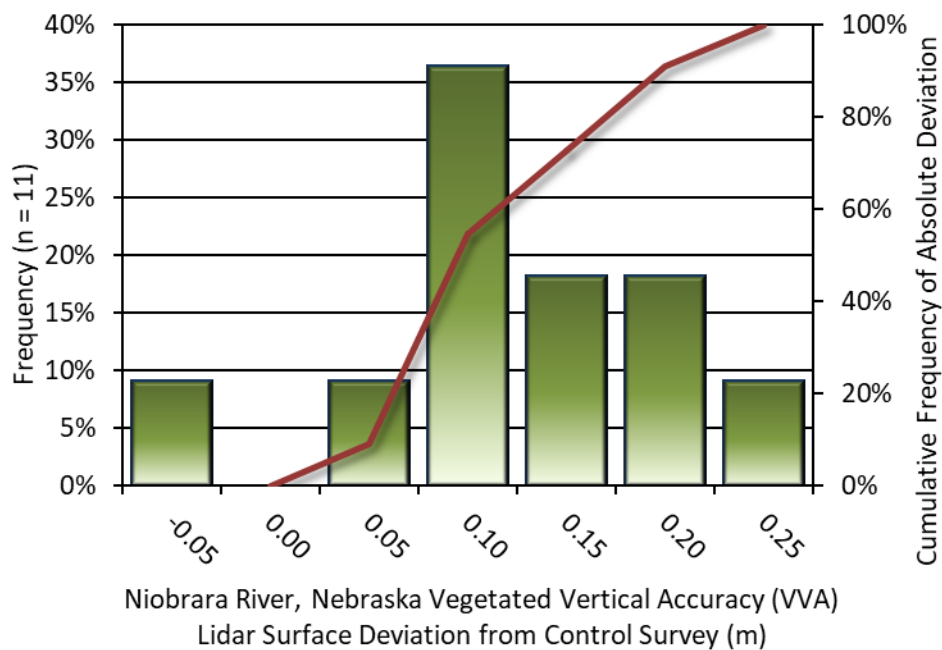Lidar Surface Deviation from Control Survey (m)

Figure 16: Frequency histogram for lidar surface deviation from all land cover class point values (VVA)
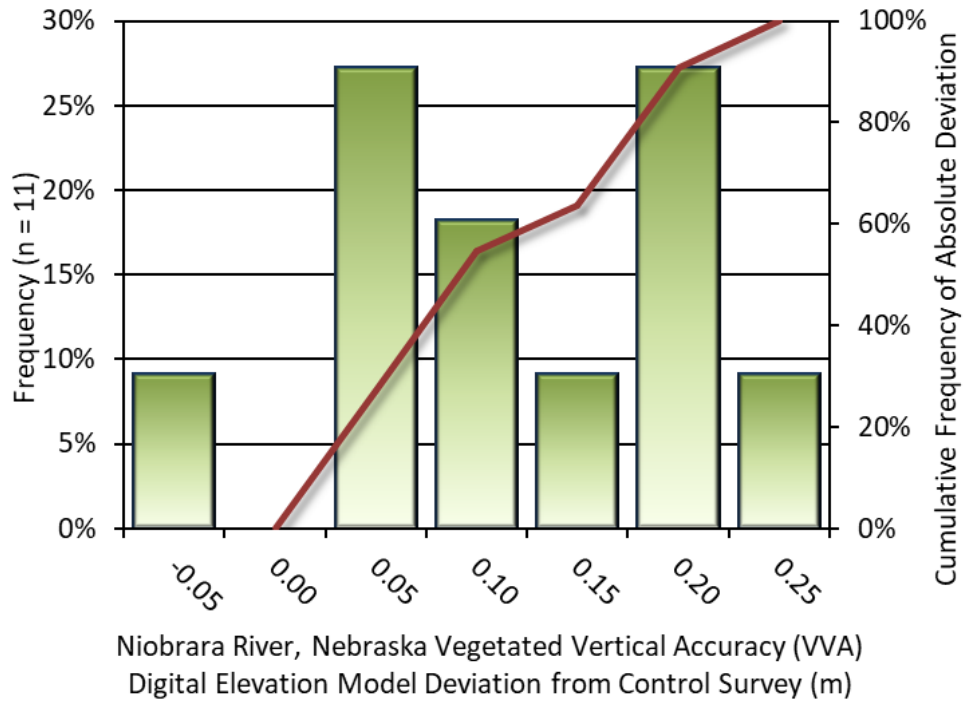
Figure 17: Frequency histogram for lidar bare earth DEM deviation from all land cover class point values (VVA)

Lidar Relative Vertical Accuracy

Relative vertical accuracy refers to the internal consistency of the data set as a whole: the ability to place an object in the same location given multiple flight lines, GPS conditions, and aircraft attitudes. When the lidar system is well calibrated, the swath-to-swath vertical divergence is low (<0.10 meters). The relative vertical accuracy was computed by comparing the ground surface model of each individual flight line with its neighbors in overlapping regions. The average (mean) line to line relative vertical accuracy for the Niobrara River Lidar project was 0.031 meters (Table 18, Figure 18).

Table 18: Relative accuracy results

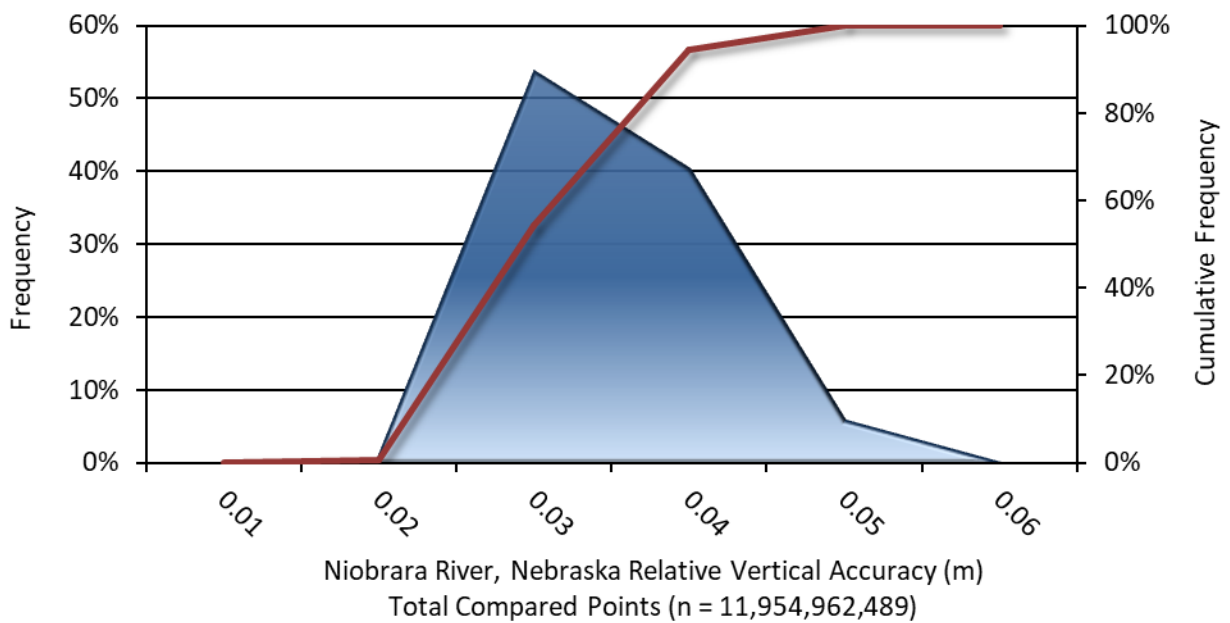| Relative Accuracy	
Sample	371 flight line surfaces
Average	0.031 m
Median	0.030 m
RMSE	0.031 m
Standard Deviation (1σ)	0.005 m
1.96σ	0.009 m

Figure 18: Frequency plot for relative vertical accuracy between flight lines

Lidar Horizontal Accuracy

Lidar horizontal accuracy is a function of Global Navigation Satellite System (GNSS) derived positional error, flying altitude, and INS derived attitude error. The obtained $RMSE_r$ value is multiplied by a conversion factor of 1.7308 to yield the horizontal component of the National Standards for Spatial Data Accuracy (NSSDA) reporting standard where a theoretical point will fall within the obtained radius 95 percent of the time. Based on a flying altitude of 400 meters, an IMU error of 0.003 decimal degrees, and a GNSS positional error of 0.015 meters, this project was compiled to meet 0.07 m horizontal accuracy at the 95% confidence level.

Table 19: Horizontal Accuracy

Horizontal Accuracy	
$RMSE_r$	0.04 m
ACC_r	0.07 m

NV5 Geospatial, Inc. provided lidar services for the Niobrara River project as described in this report.

I, Steven Miller, have reviewed the attached report for completeness and hereby state that it is a complete and accurate report of this project.
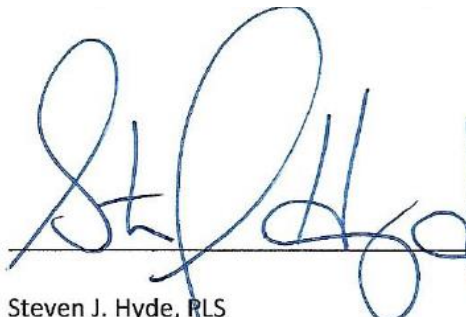
May 12, 2021

Steven Miller
Project Manager
NV5 Geospatial, Inc.

I, Steven J. Hyde, PLS, being duly registered as a Professional Land Surveyor in and by the state of Nebraska, hereby certify that the methodologies, static GNSS occupations used during airborne flights, and ground survey point collection were performed using commonly accepted Standard Practices. Field work conducted for this report was conducted between August 22nd and August 28th, 2020.

Accuracy statistics shown in the Accuracy Section of this Report have been reviewed by me and found to meet the "National Standard for Spatial Data Accuracy".

Steven J. Hyde, PLS
NV5 Geospatial, Inc.

Figure 19: View looking northwest towards a bridge over the Niobrara River. The image was created from the lidar bare earth model overlaid with the above-ground point cloud.
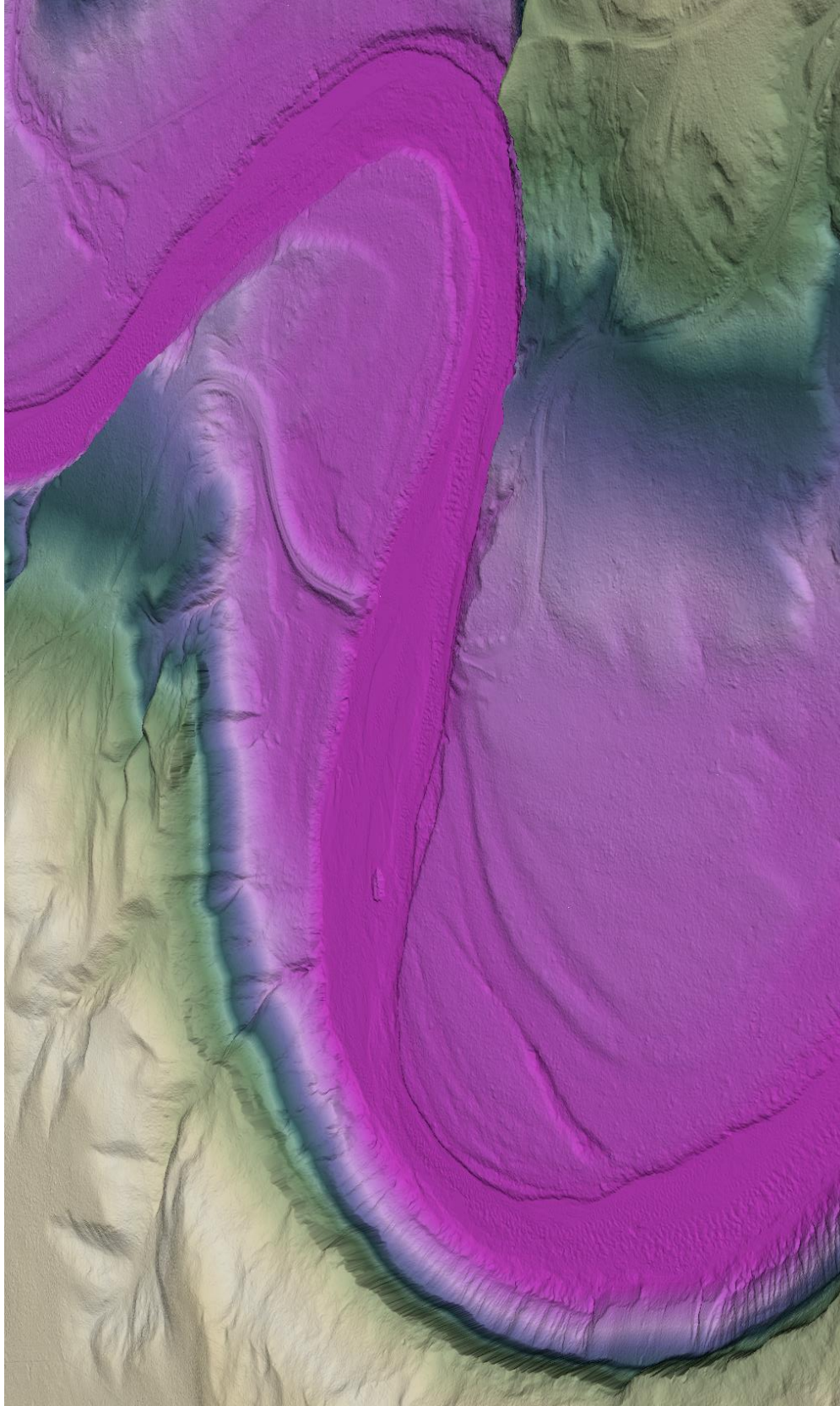
Figure 20: This view of the Niobrara River topobathymetric bare earth model is colored by elevation using a brighter color palette.

1-sigma (σ) Absolute Deviation: Value for which the data are within one standard deviation (approximately 68th percentile) of a normally distributed data set.

1.96 * RMSE Absolute Deviation: Value for which the data are within two standard deviations (approximately 95th percentile) of a normally distributed data set, based on the FGDC standards for Non-vegetated Vertical Accuracy (FVA) reporting.

Accuracy: The statistical comparison between known (surveyed) points and laser points. Typically measured as the standard deviation (sigma σ) and root mean square error (RMSE).

> **Absolute Accuracy:** The vertical accuracy of lidar data is described as the mean and standard deviation (sigma σ) of divergence of lidar point coordinates from ground survey point coordinates. To provide a sense of the model predictive power of the dataset, the root mean square error (RMSE) for vertical accuracy is also provided. These statistics assume the error distributions for x, y and z are normally distributed, and thus we also consider the skew and kurtosis of distributions when evaluating error statistics.

> **Relative Accuracy:** Relative accuracy refers to the internal consistency of the data set; i.e., the ability to place a laser point in the same location over multiple flight lines, GPS conditions and aircraft attitudes. Affected by system attitude offsets, scale and GPS/IMU drift, internal consistency is measured as the divergence between points from different flight lines within an overlapping area. Divergence is most apparent when flight lines are opposing. When the lidar system is well calibrated, the line-to-line divergence is low (<10 cm).

> **Root Mean Square Error (RMSE):** A statistic used to approximate the difference between real-world points and the lidar points. It is calculated by squaring all the values, then taking the average of the squares and taking the square root of the average.

Data Density: A common measure of lidar resolution, measured as points per square meter.

Digital Elevation Model (DEM): File or database made from surveyed points, containing elevation points over a contiguous area. Digital terrain models (DTM) and digital surface models (DSM) are types of DEMs. DTMs consist solely of the bare earth surface (ground points), while DSMs include information about all surfaces, including vegetation and man-made structures.

Intensity Values: The peak power ratio of the laser return to the emitted laser, calculated as a function of surface reflectivity.

Nadir: A single point or locus of points on the surface of the earth directly below a sensor as it progresses along its flight line.

Overlap: The area shared between flight lines, typically measured in percent. 100% overlap is essential to ensure complete coverage and reduce laser shadows.

Pulse Rate (PR): The rate at which laser pulses are emitted from the sensor; typically measured in thousands of pulses per second (kHz).

Pulse Returns: For every laser pulse emitted, the number of wave forms (i.e., echoes) reflected back to the sensor. Portions of the wave form that return first are the highest element in multi-tiered surfaces such as vegetation. Portions of the wave form that return last are the lowest element in multi-tiered surfaces.

Real-Time Kinematic (RTK) Survey: A type of surveying conducted with a GPS base station deployed over a known monument with a radio connection to a GPS rover. Both the base station and rover receive differential GPS data and the baseline correction is solved between the two. This type of ground survey is accurate to 1.5 cm or less.

Post-Processed Kinematic (PPK) Survey: GPS surveying is conducted with a GPS rover collecting concurrently with a GPS base station set up over a known monument. Differential corrections and precisions for the GNSS baselines are computed and applied after the fact during processing. This type of ground survey is accurate to 1.5 cm or less.

Scan Angle: The angle from nadir to the edge of the scan, measured in degrees. Laser point accuracy typically decreases as scan angles increase.

Native Lidar Density: The number of pulses emitted by the lidar system, commonly expressed as pulses per square meter.

Relative Accuracy Calibration Methodology:

Manual System Calibration: Calibration procedures for each mission require solving geometric relationships that relate measured swath-to-swath deviations to misalignments of system attitude parameters. Corrected scale, pitch, roll and heading offsets were calculated and applied to resolve misalignments. The raw divergence between lines was computed after the manual calibration was completed and reported for each survey area.

Automated Attitude Calibration: All data was tested and calibrated using TerraMatch automated sampling routines. Ground points were classified for each individual flight line and used for line-to-line testing. System misalignment offsets (pitch, roll and heading) and scale were solved for each individual mission and applied to respective mission datasets. The data from each mission were then blended when imported together to form the entire area of interest.

Automated Z Calibration: Ground points per line were used to calculate the vertical divergence between lines caused by vertical GPS drift. Automated Z calibration was the final step employed for relative accuracy calibration.

Lidar accuracy error sources and solutions:

Type of Error	Source	Post Processing Solution
GPS (Static/Kinematic)	Long Base Lines	None
	Poor Satellite Constellation	None
	Poor Antenna Visibility	Reduce Visibility Mask
Relative Accuracy	Poor System Calibration	Recalibrate IMU and sensor offsets/settings
	Inaccurate System	None
Laser Noise	Poor Laser Timing	None
	Poor Laser Reception	None
	Poor Laser Power	None
	Irregular Laser Shape	None

Operational measures taken to improve relative accuracy:

Low Flight Altitude: Terrain following was employed to maintain a constant above ground level (AGL). Laser horizontal errors are a function of flight altitude above ground (about 1/3000th AGL flight altitude).

Focus Laser Power at narrow beam footprint: A laser return must be received by the system above a power threshold to accurately record a measurement. The strength of the laser return (i.e., intensity) is a function of laser emission power, laser footprint, flight altitude and the reflectivity of the target. While surface reflectivity cannot be controlled, laser power can be increased and low flight altitudes can be maintained.

Reduced Scan Angle: Edge-of-scan data can become inaccurate. The scan angle was reduced to a maximum of ±20-21° from nadir, creating a narrow swath width and greatly reducing laser shadows from trees and buildings.

Quality GPS: Flights took place during optimal GPS conditions (e.g., 6 or more satellites and PDOP [Position Dilution of Precision] less than 3.0). Before each flight, the PDOP was determined for the survey day. During all flight times, a dual frequency DGPS base station recording at 1 second epochs was utilized and a maximum baseline length between the aircraft and the control points was less than 13 nm at all times.

Ground Survey: Ground survey point accuracy (<1.5 cm RMSE) occurs during optimal PDOP ranges and targets a minimal baseline distance of 4 miles between GPS rover and base. Robust statistics are, in part, a function of sample size (n) and distribution. Ground survey points are distributed to the extent possible throughout multiple flight lines and across the survey area.

50% Side-Lap (100% Overlap): Overlapping areas are optimized for relative accuracy testing. Laser shadowing is minimized to help increase target acquisition from multiple scan angles. Ideally, with a 50% side-lap, the nadir portion of one flight line coincides with the swath edge portion of overlapping flight lines. A minimum of 50% side-lap with terrain-followed acquisition prevents data gaps.

Opposing Flight Lines: All overlapping flight lines have opposing directions. Pitch, roll and heading errors are amplified by a factor of two relative to the adjacent flight line(s), making misalignments easier to detect and resolve.